Jan ZWOLAK[*], Martyna MAREK[**]

THE ANALYSIS OF THE SLIPPAGE AND CONTACT STRESS IN THE MESHING OF THE POWER-SHIFT TYPE GEAR

ANALIZA POŚLIZGU MIĘDZYZĘBNEGO I NAPRĘŻEŃ KONTAKTOWYCH W ZAZĘBIENIU KÓŁ PRZEKŁADNI ZĘBATEJ TYPU POWER SHIFT

Key words:

gear meshing, slippage, contact stress, numerical tests, optimization

Słowa kluczowe:

zazębienie kół zębatych, poślizg międzyzębny, naprężenia kontaktowe, badania numeryczne, optymalizacja

Abstract

This work is an analysis of gear slippage and contact stresses in toothed gears of a six-shaft power shift gearing. Gear meshing contains 5 characteristic contact points located within the active surface of a tooth. The contact points are as follows: A – beginning of a tooth involute profile located within double-tooth engagement area; B – the end-point of double-tooth engagement constituting the beginning of single-tooth engagement area; C – pitch point, referred to also as the central contact point; D – the last point of the single-tooth engagement

[*] University of Rzeszów, al. Rejtana 16a, 35-959 Rzeszów, Poland, tel. 17 851-85-82.
[**] Liugong Dressta Machinery, ul. Kwiatkowskiego 1, 37-450 Stalowa Wola, Poland, tel. 15 813-62-84.

being at the same time the starting point of the double-tooth engagement area, which is a part of the tooth tip; and, E – point at the tooth tip that closes the double-tooth engagement area.

The location of individual contact points and the resulting slippage and contact stress values depend on the geometrical parameters of cooperating gear wheels. The inter-relationship suggests that, in power shift gearings, the contact points have as many positions within the active surface as there are cooperating gear wheels.

INTRODUCTION

Power shift gearings can be found in power transmission systems for contemporary mobile engineering machines **[L. 1–4]**. Toothed gears in such a gearing remain in constant engagement, and a change of a gear is done with special clutches, integrated with appropriate toothed gears. The special clutches, also referred to as "wet plate clutches" **[L. 2, 5]** are comprised of alternately positioned friction and steel disks. The friction disks with internal splines are connected with the toothed gear, while the steel disks with external splines connect the shaft through a clutch basket equipped with an internal spline.

Without load, there is a gap between friction and steel disks, which disallows transferring the torque from the shaft to the toothed gear. The clutch becomes activated (i.e. turned on) when the friction and steel disks are pressed against each other by the hydraulic cylinder located within the clutch.

Discussion over the contact stresses and slippage within individual stages of a gearing requires a determination of appropriate pairs of toothed gears that form a kinematic chain, which accomplishes a given gear ratio. An engineer has to select the geometrical parameters that guarantee minimal contact stresses and slippage during the torque transfer. This problem can be solved by using computer calculation methods with multi-criterion optimisation.

GENERAL CHARACTERISTICS OF THE RESEARCH SUBJECT

Analysis of contact stresses and slippage was done on a six-shaft power shift gearing **[L. 2, 11, 12]**. The location of toothed gears within shafts provides 7-toothed pairs of the kinematic chain starting from the input shaft "I" to the output on shaft "V." Gear ratios are secured by clutches S_p, S_w, S_1, S_2, and S_3, which are integrated with toothed gears z_1, z_2, z_6, z_8, and z_{10}. **Figure 1** presents the kinematic scheme of the power shift gearing in axial alignment.

Shaft axes from I to V are positioned in 4 vertical planes. Therefore, in order to illustrate all engaged gearings, they were presented in a radial alignment in **Figure 2**.

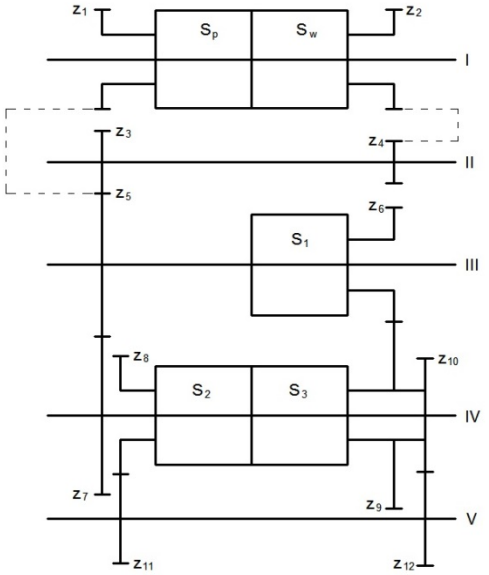

Fig. 1. Kinematic scheme of a gearing in axial alignment: $z_1 – z_{12}$ – toothed gears, S_p, S_w, S_1, S_2, S_3 – clutches, I – V – shafts

Rys. 1. Schemat kinematyczny przekładni zębatej w układzie osiowym: $z_1 \div z_{12}$ – koła zębate, S_p, S_w, S_1, S_2, S_3 – sprzęgła, I ÷ V – wały

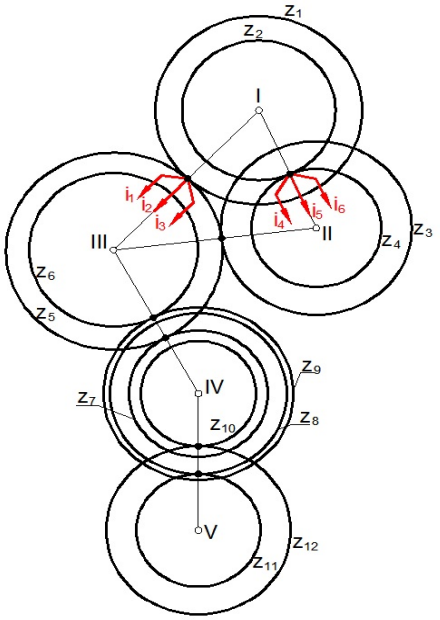

Fig. 2. Radial alignment of the researched gearing

Rys. 2. Układ promieniowy badanej przekładni zębatej

Figures 1 and **2** illustrate that it is possible to create kinematic chains that secure forward motion of a vehicle by way of activating clutch S_p integrated with toothed gear z_1, and the backward motion by way of activating clutch S_w integrated with toothed gear z_2. Other possible gear ratios (gears) can be reached by creating kinematic chains in line with the following:

Forward movement

$$i_1 = \frac{z_5}{z_1} \bullet \frac{z_9}{z_6} \bullet \frac{z_{12}}{z_{10}}$$

$$i_2 = \frac{z_5}{z_1} \bullet \frac{z_7}{z_5} \bullet \frac{z_{12}}{z_{10}}$$

$$i_3 = \frac{z_5}{z_1} \bullet \frac{z_7}{z_5} \bullet \frac{z_{11}}{z_8}$$

Backward movement

$$i_4 = \frac{z_4}{z_2} \bullet \frac{z_5}{z_3} \bullet \frac{z_9}{z_6} \bullet \frac{z_{12}}{z_{10}}$$

$$i_5 = \frac{z_4}{z_2} \bullet \frac{z_5}{z_3} \bullet \frac{z_7}{z_5} \bullet \frac{z_{12}}{z_{10}}$$

$$i_6 = \frac{z_4}{z_2} \bullet \frac{z_5}{z_3} \bullet \frac{z_7}{z_5} \bullet \frac{z_{11}}{z_8}$$

where: $i_1,\ldots,i_6$ are the gear ratios for appropriate gears. It can be noticed that toothed gear z_5 forms a toothed pair with gear z_1 as well as with gear z_7 and gear z_3. Therefore, the toothed gear z_5 suffers the highest amount of load cycles in the given time of operation. Characteristic contact points: E_1, E_2, B_1, B_2, C, which are present in all toothed pairs **[L. 6**,7**]**, are presented in **Figures 3** and **4**.

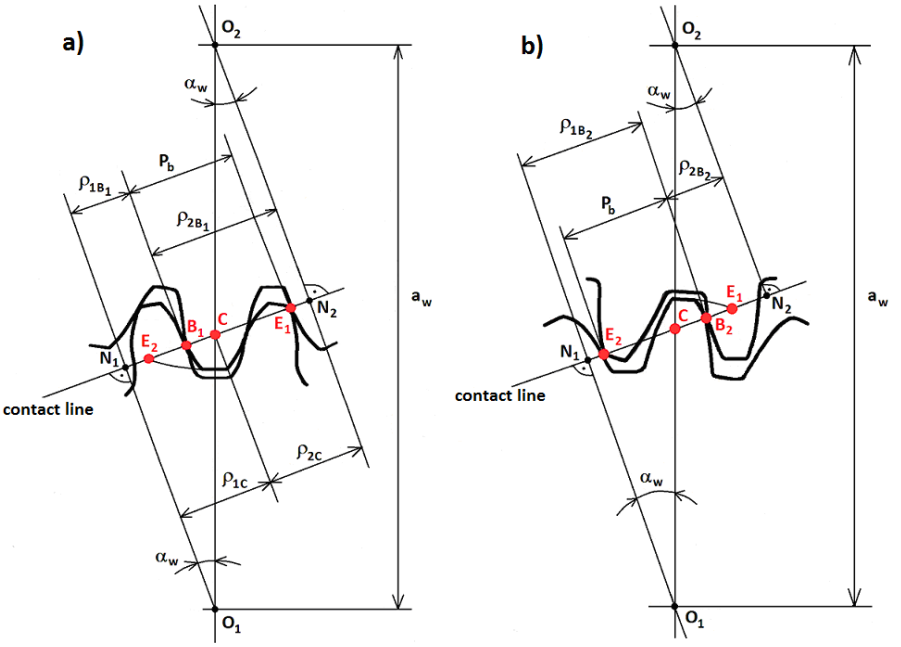

Fig. 3. Toothed pair with the following tooth engagement area: a) B_1E_1, b) B_2E_2
Rys. 3. Para zębata z odcinkiem zazębienia: a) B_1E_1, b) B_2E_2

Figure 3a illustrates how the operation of one toothed pair starts in point B_1, while the operation of the other toothed pair finishes in point E_1. **Figure 3b** illustrates point B_2, where: one toothed pair finishes its operation, and the point E_2, where: other toothed pair begins its operation. It was assumed that the drive gear with centre O_1 rotates clockwise in order to determine the characteristic points.

The remaining geometrical parameters illustrated in **Figures 3a** and **3b**, which impact contact stress and slippage values, adopt the following meaning: ρ_{1B1} – curvature radius of involute profile for tooth in gear 1 within point B_1, ρ_{2B1} – curvature radius of involute profile for tooth in gear 2 within point B_1, p_b – principle scale, ρ_{1C} – curvature radius of involute profile for tooth in gear 1 within point C, ρ_{2C} – curvature radius of involute profile for tooth in gear 2 within point C, ρ_{1B2} – curvature radius of involute profile for tooth in gear 1 within point B_2, ρ_{2B2} – curvature radius of involute profile for tooth in gear 2 within point B_2, a_w – actual distance between axis of toothed gear 1 and toothed gear 2, and α_w – rolling pressure angle. Location of curvature radii for the involute profile of a toothed pair within various points **[L. 6, 7, 13]** was presented in **Figure 4**.

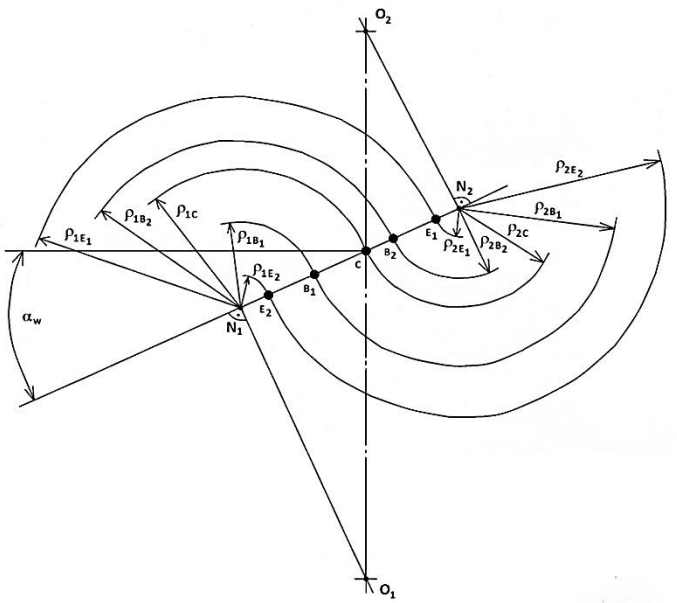

Fig. 4. The contact line and curvature radii of characteristic contact points in a toothed pair

Rys. 4. Linia przyporu i promienie krzywizny charakterystycznych punktów styku pary zębatej

Point N_1 is the point of contact between the contact line and the principle circle of the toothed gear with centre O_1, which means that the section O_1N_1 is

the principle radius of this gear. A similar definition applies to point N_2, which refers to the toothed gear with centre O_2.

When taking advantage of **Figures 3a, 3b**, and **4**, it is possible to specify the characteristic points and then contact stress and slippage values of the gearing using the original computer software **[L. 8]**.

NUMERICAL TESTS AND RESEARCH RESULTS

Numerical tests consisted in specifying contact stresses and slippage values in characteristic points within the active surface of power shift gearing. The locations of characteristic points within the involute profile of the teeth forming the toothed pair are presented in **Figure 5**.

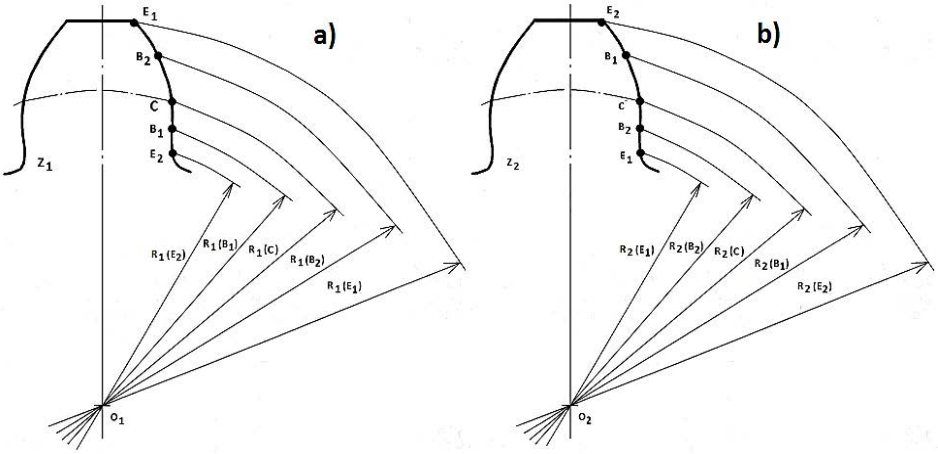

Fig. 5. Location of characteristic points: a) on the tooth of the drive gear, b) on the tooth of the driven gear

Rys. 5. Położenie punktów charakterystycznych: a) na zębie koła napędzającego i b) na zębie koła napędzanego

The definition of points located over the engagement area, referred to as the characteristic points, are as follows: E_2 – beginning of the active profile within the propelling tooth root, B_1 – internal point of single-tooth engagement, C – central point of engagement (the pitch point), B_2 – external point of single-tooth engagement, and E_1 – the end of active profile within the tip of the propelling tooth.

It is worth noticing that engagement between gear z_1 (**Fig. 5a**) and gear z_2 (**Fig. 5b**) cause the following points to overlap: $E_1 = E_2$, $B_2 = B_1$, C = C, $B_1 = B_2$, and $E_2 = E_1$. As shown in **Figures 4** and **5**, part of the involute profile concerning teeth E_1B_2 and E_2B_1 at their tip in the toothed pair is located in double-tooth engagement. Part of the B_1E_2 and B_2E_1 profiles near the base of the

toothed pair are located in the double-tooth engagement as well. The middle part of B_2B_1 and B_1B_2 tooth profile is located within single-tooth engagement.

Geometrical and operation parameters were defined by using an original computer software **[L. 8]**. The software was developed on the basis of an algorithm, which employs formulas contained within the international standard ISO – 6336 **[L. 9]** and available literature **[L. 10**, **14, 15, 16]**. Thus, this work will not include any detailed formulas.

Hence, after multi-criterion optimisation, only results for contact stress and slippage values are presented **[L. 17, 18]** in characteristic points within the active surface. The software conducts optimisation with 11 criteria, which include the maximum number of contact points, minimal tooth shape coefficient, minimal thickness at the tooth tip, the total weight of toothed gears, the total mass inertial moment of toothed gears, the maximal durability of tooth root and tooth edge, material effort uniformity within toothed gears, the minimal relative thickness of the oil film within the area between teeth, gearing efficiency, and minimal slippage value.

Due to a large volume of results obtained for 5 characteristic contact points in all toothed pairs that constitute the tested gearing, the current author will focus on providing slippage values only for the extreme points E_1 and E_2. In those points, the slippage values take maximum levels at the engagement area, which was illustrated in **Table 1**.

Table 1. Slippage velocity values within the active surface following the 1st calculations
Tabela 1. Wartości prędkości poślizgów na wysokości czynnej zębów po 1 kroku obliczeń

Gear	Toothed pair							Contact point
	z_1/z_5	z_6/z_9	z_{10}/z_{12}	z_5/z_7	z_8/z_{11}	z_2/z_4	z_3/z_5	
I	4.317	3.185	2.320					E_1
II	4.317		3.972	3.759				
III	4.317			3.759	5.613			
IV		3.185	2.320			5.260	4.340	
V			3.972	3.759		5.260	4.340	
VI				3.759	5.613	5.260	4.340	
I	4.295	3.182	2.081					E_2
II	4.295		3.563	4.298				
III	4.295			4.298	5.702			
IV		3.182	2.081			5.260	4.272	
V			3.563	4.298		5.260	4.272	
VI				4.298	5.702	5.260	4.272	

The slippage values in **Table 1** [m × s^{-1}] are the results obtained in the 1st step of calculations before optimisation. The empty fields in **Table 1** denote that the given toothed pair does not take part in the torque transfer.

The conducted optimisation calculations, based on previously mentioned 11 criteria, illustrate slippage values for contact points E_1 and E_2, as shown in **Table 2**.

Table 2. Slippage velocity values within the active surface following optimisation
Tabela 2. Wartości prędkości poślizgów na wysokości czynnej zębów po optymalizacji

Gear	Toothed pair							Contact point
	z_1/z_5	z_6/z_9	z_{10}/z_{12}	z_5/z_7	z_8/z_{11}	z_2/z_4	z_3/z_5	
I	4.187	1.726	2.507					E_1
II	4.187		3.030	2.579				
III	4.187			2.579	5.242			
IV		1.380	2.004			3.406	3.480	
V			2.422	2.062		3.406	3.480	
VI				2.062	4.191	3.406	3.480	
I	3.202	3.751	2.197					E_2
II	3.202		2.656	4.076				
III	3.202			4.076	3.073			
IV		2.999	1.756			3.866	2.315	
V			2.123	3.258		3.866	2.315	
VI				3.258	2.456	3.866	2.315	

As far as durability against fatigue within surfaces of the toothed gears is concerned, the primary attention should be paid to contact stresses that result from torque transfer. Similarly as in the case of slippage values, the contact points E_1 and E_2 along with corresponding contact stress values were selected after the first step of calculations (**Table 3**).

Table 3. Contact stress values [MPa] following 1st step of calculations
Tabela 3. Wartości naprężeń kontaktowych [MPa] po 1 kroku obliczeń

Gear	Toothed pair							Contact point
	z_1/z_5	z_6/z_9	z_{10}/z_{12}	z_5/z_7	z_8/z_{11}	z_2/z_4	z_3/z_5	
I	713.2	1161.0	761.8					E_1
II	713.2		582.5	856.3				
III	713.2			856.3	1146.4			
IV		1161.0	761.8			833.3	901.6	
V			582.5	856.3		833.3	901.6	
VI				856.3	1146.4	833.3	901.6	
I	793.9	1292.4	848.0					E_2
II	793.9		648.4	953.2				
III	793.9			953.2	1276.2			
IV		1292.4	848.0			927.7	1003.7	
V			648.4	953.2		927.7	1003.7	
VI				953.2	1276.2	927.7	1003.7	

Table 4 illustrates the values of contact stresses obtained after multi-criterion optimisation conducted by way of specifying 11 criteria.

Table 4. Contact stress values [MPa] following optimisation
Tabela 4. Wartości naprężeń kontaktowych [MPa] po optymalizacji

Gear	Toothed pair							Contact point
	z_1/z_5	z_6/z_9	z_{10}/z_{12}	z_5/z_7	z_8/z_{11}	z_2/z_4	z_3/z_5	
I	928.6	1205.2	880.6					E_1
II	928.6		800.8	1196.3				
III	928.6			1196.3	1192.4			
IV		1347.5	984.6			907.8	980.2	
V			895.3	1337.5		907.8	980.2	
VI				1337.5	1333.1	907.8	980.2	
I	1027.3	1333.3	974.2					E_2
II	1027.3		885.9	1323.4				
III	1027.3			1323.4	1319.1			
IV		1490.7	1089.2			1004.2	1084.4	
V			990.5	1479.6		1004.2	1084.4	
VI				1479.6	1474.8	1004.2	1084.4	

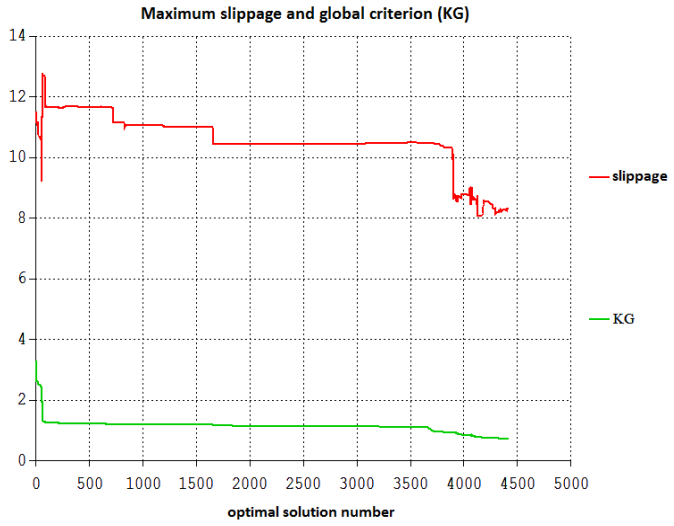

Fig. 6. The example of decreasing slippage over subsequent optimisation steps
Rys. 6. Przykład malejącego poślizgu w kolejnych krokach optymalizacji

From among 11 criteria, which served as a basis for the optimisation described in this work, the current author paid special attention to slippage and

contact stress values. However, the global criterion refers to all of the 11 criteria. **Figure 6** presents the slippage chart compared with the global criterion.

In multi-criterion optimisation, the main objective consists in achieving the lowest global criterion K_G at which it is assumed that the investigated problem has been optimally solved according to all developed criteria. The chart presents changes in slippage values from about 12 m × s^{-1} to about 8 m × s^{-1} at global criterion below 1 (obtained after almost 4000 optimisation steps).

Among many other criteria being calculated, **Figure 7** will focus on illustrating the changing value of contact stresses.

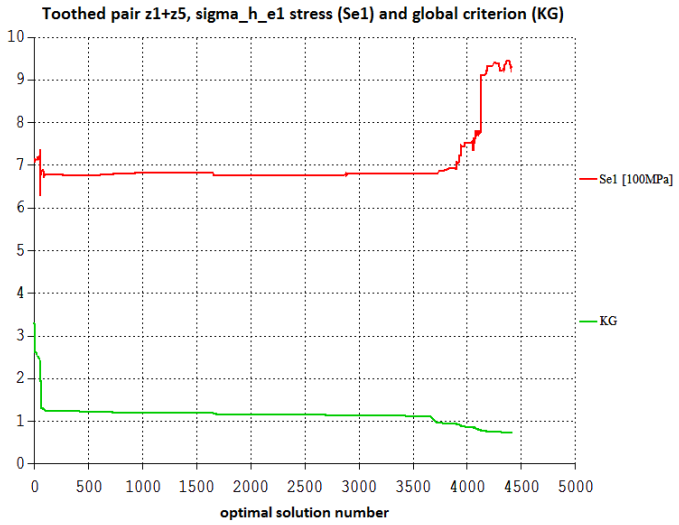

Fig. 7. Increasing contact stresses over subsequent optimisation steps
Rys. 7. Wzrastające naprężenia kontaktowe w kolejnych krokach optymalizacji

The red curve defines contact stresses of the z_1+z_5 toothed pair on gear 2 within the contact point E_1. In case of slippage, the lowest value was obtained after about 4000 steps of optimisation, while under stress, their value increases. It is possible through the value of fatigue contact durability σ_{Hlim} **[L. 19]** that has been entered into the PRZEKŁADNIA software **[L. 8]**. In order to obtain actual contact stress values, the values presented in the chart should be multiplied by 100 MPa.

The contact stress line in 5 characteristic points within the active surface is presented in **Figure 8**.

Contact stress lines at the contact points: E_1, B_2, C, B_1, E_2 suggest that the increase in their value takes place after about 4000 optimisation steps.

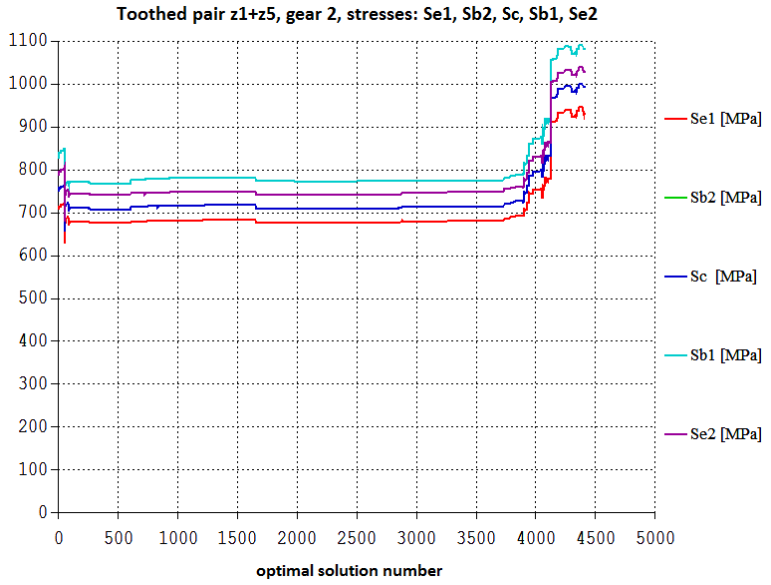

Fig. 8. Contact stresses at 5 characteristic points
Rys. 8. Naprężenia kontaktowe w 5 charakterystycznych punktach

ANALYSIS OF THE RESULTS

In the conducted optimisation research of a 6-shaft power shift gearing that took place according to 11 criteria, the analysis focused on two: slippage and contact stress values. Those criteria, except for other conditions, should be taken into account by the engineer at the gearing design stage. For selected slippage and contact stress values, the software calculates all geometrical and durability parameters of individual toothed gears that meet conditions specified by the engineer at the stage of creating the optimisation sequence.

In case of this toothed pair (z_1+z_5), the optimal solution will be reached after about 4000 steps of optimisation. **Figures 6, 7,** and **8** illustrate that such number of calculations leads to a lowered slippage and elevated contact stresses. This is proved by a decrease in the global criterion value, which falls below 1.0. In actual gearings, the main objective is to guarantee the lowest slippage values possible, while the operating contact stress should correspond to fatigue contact durability σ_{Hlim}, which, for SAE 8620 steel, equals 1492 MPa. **Figure 8** presents toothed pair z_1+z_5, which suffers contact stresses from 700 to 1100 MPa. Therefore, there is a great room for applying various materials within the scope of fatigue contact durability.

SUMMARY AND CONCLUSIONS

The conducted analysis with multi-criterion optimisation of the power shift gearing showed that the first stage being a toothed pair z_1+z_5 is characterized by geometrical parameters at which the contact stresses are too low. This means that durability of the materials is not fully utilised.

The calculated contact stress values within contact point E_2 at the tooth root reach the highest levels; therefore, this is the area around which the pitting will occur in the first place. This is confirmed by experimental tests.

Slippage between teeth in given toothed pairs should be kept minimized due to friction processes and the resulting high amounts of heat. Such calculations with or without optimisation are possible with the help of PRZEKŁADNIA *[in English: GEARBOX]* computer software.

In the central contact point C, the slippage value equals zero, because the tangential velocities in this contact point for gears z_1 and z_5 are equal.

REFERENCES

1. Park S.M., Park T.W., Lee S.H., Han S.W., Kwon S.K.: Analytical study to estimate the performance of the power shift drive axle for a forklift. International Journal of Automotive Technology, vol. 11, 2010.
2. Materiały firmowe Huty Stalowa Wola, 2014.
3. Molari G., Sedoni E.: Experimental evaluation of power losses in a power shift agricultural tractor transmission. Biosystems Engineering, vol. 100, June 2008.
4. Tanelli M., Panzaui G., Savaresi S.M., Pirola C.: Transmission control for power shift agricultural tractors. Mechatronics, vol. 21, February 2011.
5. Zwolak J.: Analiza olejowego układu przepływowego i jakości smarowania tarcz sprzęgłowych w przekładniach zębatych power shift. Tribologia, nr 4, 2014.
6. Muller L.: Przekładnie zębate. WNT, Warszawa 1996.
7. Pedrero J.I., Pleguezuelos M., Artes M., Antona J.A.: Load distribution model along the line of contact for involute external gears. Mechanism and Machine Theory, vol. 45, 2010.
8. Martyna M., Zwolak J.: Program komputerowy z optymalizacją wielokryterialną PRZEKŁADNIA. www.gearbox.com.pl.
9. ISO Standard 6336, 1996: Calculation of load capacity of spur and helical gears.
10. Jabbour T., Asmar G.: Tooth stress calculation of metal spur and helical gears. Mechanism and Machine Theory, vol. 92, October 2015.
11. Yegen I., Usta M.: The effect of salt bath cementation on mechanical behavior of hot-rolled and cold-drawn SAE 8620 and 16MnCr5 steels. Vacuum, vol. 85, 2010.
12. Osman T., Velex Ph.: A model for the simulation of the interactions between dynamic tooth loads and contact fatigue in spur gears. Tribology International, vol. 46, 2012.
13. Amarnath M., Sujatha C., Swarnamani S.: Experimental studies on the effects of reduction in gear tooth stiffness and lubricant film thickness in a spur geared system. Tribology International, vol. 42, 2009.

14. Sanchez M.B., Pedrero J.I., Pleguezuelos M.: Contact stress calculation of high transverse contact ratio spur and helical gear teeth. Mechanism and Machine Theory, vol. 64, June 2013.
15. Pedrero J.I., Pleguezuelos M., Munoz M.: Contact stress calculation of undercut spur and helical gear teeth. Mechanism and Machine Theory, vol. 46, November 2011.
16. Tuszyński W., Michalczewski R., Szczerek M., Kalbarczyk M.: A new scuffing shock test method for the determination of the resistance to scuffing of coated gears. Archives of Civil and Mechanical Engineering, vol. 12, December 2012.
17. Bobach L., Beilicke R., Bartel D., Deters L.: Thermal elastohydrodynamic simulation of involute spur gears incorporating mixed friction. Tribology International, vol. 48, 2012.
18. Li B., Sansavini G.: Effective multi-objective selsction of inter-subnetwork power shifts to mitigate cascading failures. Electric Power Systems Research, vol. 134, May 2016.
19. Zwolak J., Palczak A.: The effect of the gear teeth finishing method on the properties of the teeth surface layer and its resistance to the pitting wear creation. Journal of Central South Uniwersity, vol. 23, issue 1, January 2016.

Streszczenie

W pracy przeprowadzono analizę poślizgu międzyzębnego i naprężeń kontaktowych kół zębatych w 6-stopniowej przekładni power shift. W zazębieniu kół zębatych wyróżniono 5 charakterystycznych punktów przyporu występujących na wysokości czynnej zęba. Punktami tymi są: A – początek czynnego zarysu ewolwentowego zęba należący do strefy dwuparowego zazębienia, B – punkt końca strefy dwuparowego zazębienia będący równocześnie początkiem strefy jednoparowego zazębienia, C – biegun zazębienia zwany też centralnym punktem zazębienia, D – punkt końca strefy jednoparowego zazębienia, a rozpoczynający strefę dwuparowego zazębienia należącą do głowy zęba, E – punkt na wierzchołku zęba zamykający strefę dwuparowego zazębienia.

Położenie poszczególnych punktów przyporu, a wraz z tym wartości poślizgu i naprężeń kontaktowych uzależnione jest od parametrów geometrycznych kół współpracujących. Zależności wskazują, że w przypadku przekładni power shift punkty przyporu będą miały tyle położeń na wysokości czynnej zęba, ile jest z nim kół współpracujących.